DOI: 10.1002/ejic.200700441

Tetrahedral Co^{II} Complexes with CoI_2O_2 and CoO_2S_2 Cores – Crystal Structures of $[Co\{HN(OPPh_2)(SPPh_2)\text{-}O\}_2I_2]$ and $[Co\{N(OPPh_2)(SPPh_2)\text{-}O,S\}_2]$

M. Carla Aragoni,[a] Massimiliano Arca,[a] M. Bonaria Carrea,[a] Alessandra Garau,[a] Francesco A. Devillanova,[a] Francesco Isaia,*[a] Vito Lippolis,[a] Gian Luca Abbati,[b] Francesco Demartin,[c] Cristian Silvestru,[d] Serhiy Demeshko,[e] and Franc Meyer[e]

Keywords: Cobalt / O,S ligands / Phosphanes / Sulfides / Density functional calculations / Magnetic properties

The compound $[Co^{II}\{HN(OPPh_2)(SPPh_2)\text{-}O\}_2I_2]$ (**1**) was synthesised by the reaction of cobalt in powder with the iodine adduct of tetraphenylthiooxoimidodiphosphinic acid, $HN(OPPh_2)(SPPh_2)$, in Et_2O; treatment of compound **1** with NaOH resulted in deprotonation of the ligands bound to the metal ion and a separation of $[Co^{II}\{N(OPPh_2)(SPPh_2)\text{-}O,S\}_2]$ (**2**). Molecular structures of complexes **1** and **2** were elucidated by X-ray diffraction analysis, which revealed a CoI_2O_2 tetrahedral core for compound **1** in which two neutral ligands bind through the oxygen atoms the Co^{II} ion, and a tetrahedral CoO_2S_2 core for compound **2** with the oxygen and sulfur atoms of each anionic ligand chelating a Co^{II} centre. Variable-temperature magnetic susceptibility measurements are consistent with tetrahedral high-spin ($S = 3/2$) Co^{II} that possesses a $^4A_2$ ground state with best fit parameters $g = 2.25$, $|D| = 12.0\ cm^{-1}$ and $g = 2.37$, $|D| = 11.9\ cm^{-1}$ for complexes **1** and **2**, respectively. The compounds were further characterised by UV/Vis and IR spectroscopy. DFT calculations were performed on model complexes $[Co^{II}\{N(OPH_2)(SPH_2)\text{-}O,S\}_2]$ (**3**) and $[Co^{II}\{N(SPH_2)_2\text{-}S,S'\}_2]$ (**4**) to compare the electronic properties of the CoO_2S_2 and CoS_4 cores.

Introduction

The use of iodine or interhalogen charge-transfer adducts of chalcogen donor molecules as oxidising/complexing agents towards zero-valent metals has been attracting some interest in recent years because of their applications both in the recovery of precious metals from waste industrial materials and in the recovery of toxic metals for the environment.[1] Because a great number of iodine adducts with ligands containing sulfur donor atoms have been synthesised, a wide choice of "reagents" is to be considered potentially available for the oxidation/complexation of metals.[2] However, only a few of them have really proved successful to date. Previous studies led us to consider that the overall oxidation/complexation reaction was composed of two distinct processes in which the adduct was accountable for the oxidation of the metal and the ligand/donor for the complexation of the formed metal ion.[3] On the basis of these considerations, the formation of the I_2 adduct of tetraphenyldithioimidodiphosphinic acid, $HN(SPPh_2)_2$, $HL_{(SS)}$, represents a successful attempt to join together the donor ability of the phosphane sulfide group and I_2. The result is a "robust" adduct, and the intrinsic ability of $HL_{(SS)}$ and its deprotonated form $[N(SPPh_2)_2]^-$, $L_{(SS)}$, to adapt well to the preferred coordination geometries of the metal ion results in a variety of coordination patterns mainly involving S,S′ sulfur chelation. In this respect, the reaction in diethyl ether of the $HL_{(SS)}\cdot I_2$ adduct with a variety of metal powders − Au, Co, Cu, In, Pd and Sb − and liquid Hg allowed their oxidation and the formation of complexes of the resulting metal ions with the ligand in its anionic form.[1c–1e,4] In the reaction with Hg and Cu, it was also possible to separate solid compounds whose crystal structures showed the unusual presence of $HL_{(SS)}$ in a S,S′-isobidentate coordinated fashion, i.e. complexes $[Hg\{HL_{(SS)}\}I_2]$ and $[Cu\{HL_{(SS)}\}_2]I_3$.[1d,5]

As a natural development of this synthetic route, we selected the adduct $HN(OPPh_2)(SPPh_2)\cdot I_2$, $HL_{(OS)}\cdot I_2$, as the oxidising agent on the basis of the ligand containing mixed

[a] Dipartimento di Chimica Inorganica ed Analitica, Università degli Studi di Cagliari,
S.S. 554 Bivio per Sestu, 09042 Cagliari, Italy
[b] Dipartimento di Chimica, Università di Modena e Reggio Emilia,
Via G. Campi 183, 41100 Modena, Italy
[c] Dipartimento di Chimica Strutturale e Stereochimica Inorganica, Università di Milano,
Via G. Venezian 21, 20133 Milano, Italy
[d] Facultatea de Chimie si Inginerie Chimica, Universitatea Babes-Bolyai,
400028 Cluj-Napoca, Romania
[e] Institut für Anorganische Chemie, Georg-August-Universität Göttingen,
Tammannstrasse 4, 37077 Göttingen, Germany
Supporting information for this article is available on the WWW under http://www.eurjic.org or from the author.

hard (O) and soft (S) donor atoms for better ion-complexing adaptability. The chemistry of this ligand has been studied far less than that of $HL_{(SS)}$; according to the complexes reported in the literature, chelation as an O,S-bidentate anionic ligand [$L_{(OS)}$; Scheme 1, structure I] is dominant, but not exclusive, with the S-monodentate coordination mode (Scheme 1, structure II) being adopted in a variety of complexes.[6] To date, no complexes of $HL_{(OS)}$ have been characterised by X-ray crystallographic analysis.

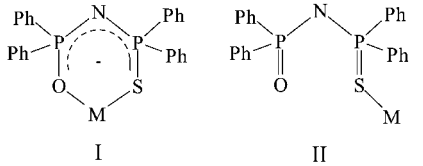

Scheme 1.

This manuscript reports the reactivity of $HL_{(OS)}$ with cobalt powder by using I_2 as the activating agent; the structures of complexes $[Co^{II}\{HN(OPPh_2)(SPPh_2)\text{-}O\}_2I_2]$ (**1**) and $[Co^{II}\{N(OPPh_2)(SPPh_2)\text{-}O,S\}_2]$ (**2**), the latter obtained by imido deprotonation of the ligands in **1**, were determined by single-crystal X-ray diffraction analysis. Magnetic parameters were also determined for both complexes. The reactivity of complex **1** towards a few soft metal ions was studied in an attempt to synthesise heterobinuclear complexes; moreover, the protonation reaction of **2** by aqueous hydroiodic acid is reported. In addition, the electronic nature of the CoO_2S_2 and CoS_4 cores was investigated by DFT calculations on model compounds $[Co^{II}\{N(OPH_2)(SPH_2)\text{-}O,S\}_2]$ and $[Co^{II}\{N(SPH_2)_2\text{-}S,S'\}_2]$.

Results and Discussion

Synthesis and Crystal Structure Determination of $[Co^{II}\{HN(OPPh_2)(SPPh_2)\text{-}O\}_2I_2]$ (1)

The reaction between equimolar amounts of the adduct $HL_{(OS)}\cdot I_2$ and Co powder was carried out under a nitrogen atmosphere in anhydrous diethyl ether. After three days of stirring, ^{31}P NMR spectroscopic resonances of the $HL_{(OS)}\cdot I_2$ species were not detectable any longer in the mixture. In the course of the reaction, the initial dark-red colour of the solution, typical of the charge-transfer adduct $HL_{(OS)}\cdot I_2$ bearing the S–I–I group, turned to light emerald green, and gradually, a light greenish powder separated from the solution. Elemental analyses of the separated powder agrees with the formed complex having stoichiometry $[Co^{II}\{HL_{(OS)}\}_2I_2]$ (**1**), and both ligand molecules are coordinated, unprecedentedly, in their neutral form, in accordance with the overall reaction in Equation (1).

$$\underset{HL_{(OS)}}{2\ HN(OPPh_2)(SPPh_2)} + I_2 + Co \xrightarrow{Et_2O} \underset{\mathbf{1}}{[CoI_2\{HN(OPPh_2)(SPPh_2)\}_2]} \quad (1)$$

Because of the different bonding modes that are inherently possible for $HL_{(OS)}$, and the unusual formulation of complex **1**, X-ray diffraction analysis was undertaken to firmly establish the coordination pattern at the cobalt centre.

The molecular structure of **1** is reported in Figure 1; selected bond lengths and angles are given in Table 1. The complex contains a tetrahedral Co^{2+} ion surrounded by two iodide anions and by two $HL_{(OS)}$ monodentate ligands coordinated to the metal atom through the oxygen atom. The tetrahedral CoO_2I_2 core is slightly distorted with a Co(1)–I(1)–I(1)/Co(1)–O(1)–O(2) dihedral angle of 84.21(7)°; the X–Co–Y (X, Y = I, O) angles are in the range 100.94(11)–

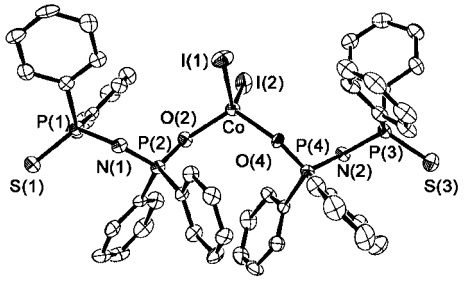

Figure 1. ORTEP drawing and atom-labelling scheme for $[Co^{II}\{HN(OPPh_2)(SPPh_2)\text{-}O\}_2I_2]$ (**1**). Thermal ellipsoids are drawn at 30% probability.

Table 1. Selected bond lengths [Å] and angles [°] for compounds **1** and **2**.

Compound **1**			
Co–O(2)	1.957(4)	Co–O(4)	1.975(4)
Co–I(1)	2.5720(8)	Co–I(2)	2.5704(8)
S(1)–P(1)	1.941(2)	S(3)–P(3)	1.934(2)
O(2)–P(2)	1.496(4)	O(4)–P(4)	1.510(4)
P(1)–N(1)	1.693(4)	P(2)–N(1)	1.642(5)
P(3)–N(2)	1.686(4)	P(4)–N(2)	1.657(5)
I(1)–Co–I(2)	118.93(3)	I(1)–Co–O(2)	108.35(11)
I(1)–Co–O(4)	100.94(11)	O(2)–Co–O(4)	113.19(15)
I(2)–Co–O(2)	102.76(11)	I(2)–Co–O(4)	113.01(11)
Co–O(2)–P(2)	141.3(2)	Co–O(4)–P(4)	144.4(2)
S(1)–P(1)–N(1)	115.6(2)	S(3)–P(3)–N(2)	114.2(2)
O(2)–P(2)–N(1)	113.8(2)	O(4)–P(4)–N(2)	114.4(2)
P(1)–N(1)–P(2)	131.2(3)	P(3)–N(2)–P(4)	129.9(3)
Compound **2**			
Co(1)–O(1)	2.003(4)	Co(1)–O(2)	1.956(4)
Co(1)–S(1)	2.3199(19)	Co(1)–S(2)	2.3426(19)
S(1)–P(1)	2.012(2)	S(2)–P(3)	2.024(2)
O(1)–P(2)	1.598(4)	O(2)–P(4)	1.526(4)
P(1)–N(1)	1.584(5)	P(3)–N(2)	1.568(5)
P(2)–N(1)	1.574(5)	P(4)–N(2)	1.591(5)
S(1)···O(1)	3.553(5)	S(2)···O(2)	3.439(4)
S(1)···S(2)	3.798(3)	O(1)···O(2)	3.159(5)
S(1)···O(2)	3.612(4)	O(1)···S(2)	3.575(4)
O(1)–Co(1)–S(1)	110.34(14)	O(2)–Co(1)–S(2)	105.93(13)
O(2)–Co(1)–S(1)	115.03(14)	O(1)–Co(1)–S(2)	110.46(13)
O(2)–Co(1)–O(1)	105.86(17)	S(1)–Co(1)–S(2)	109.09(7)
Co(1)–S(1)–P(1)	98.67(8)	Co(1)–S(2)–P(3)	95.82(8)
Co(1)–O(1)–P(2)	122.0(3)	Co(1)–O(2)–P(4)	125.4(2)
S(1)–P(1)–N(1)	118.0(2)	S(2)–P(3)–N(2)	117.10(19)
O(1)–P(2)–N(1)	118.9(2)	O(2)–P(4)–N(2)	116.8(2)
P(1)–N(1)–P(2)	133.2(3)	P(3)–N(2)–P(4)	135.5(3)

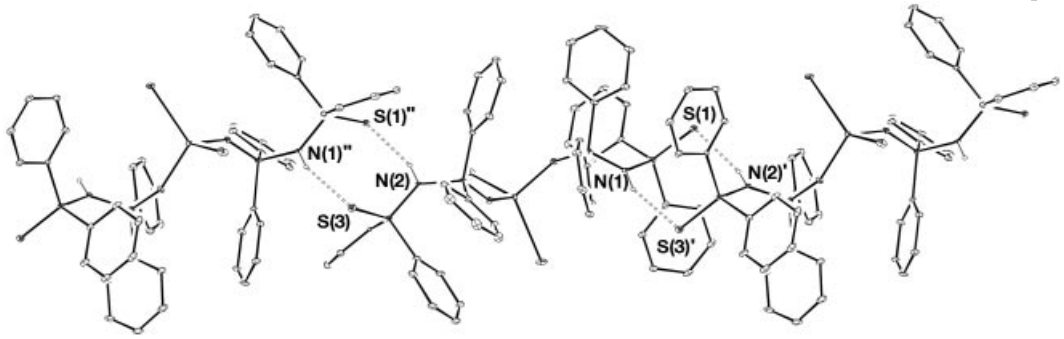

Figure 2. View of the hydrogen bonding pattern for the molecules of compound **1**.

118.93(3)°, and the Co–I and Co–O average distances are 2.5712(8) and 1.966(4) Å, respectively, (Table 1), which are very close to those reported for several monomeric Co^{II} complexes displaying tetracoordination.[7] The O and S atoms of each $HL_{(OS)}$ ligand are on opposite sides with respect to the P–N–P plane and are arranged so that the sulfur atoms are involved in S···H–N hydrogen bonding with adjacent complex molecules to form a polymeric array as shown in Figure 2; the S(1)···N(2)′ (′ = *x*, 3/2 – *y*, 1/2 + *z*) interaction is 3.365(5) Å and the N(1)···S(3)′ is 3.306(4) Å; the S1···H′–N(2)′ and N(1)–H–S(3)′ angles are 161.7 and 155.8°, respectively.

Reactivity of Complex 1 and Crystal Structure of $[Co^{II}\{N(OPPh_2)(SPPh_2)\text{-}O,S\}_2]$ (2)

The X-ray crystal structure of **1** highlights two interesting features not yet reported: (1) the neutral $HL_{(OS)}$ ligands form units within the complex and (2) the O-monodentate coordination mode at the Co^{II} centre, which leaves the $-PPh_2(S)$ groups in a dangling position. These aspects make compound **1** attractive, as further coordination towards the soft metal centre through the S donor atoms to form heterobinuclear complexes is, in principle, feasible. Moreover, the mono- or dideprotonation of the coordinated ligands in **1** may increase the nucleophilicity of the sulfur donor atoms as a consequence of the delocalisation of the negative charge(s) over the complex. First, the reactivity of **1** was tested towards a soft acceptor species such as molecular iodine, as the formation/separation of 1:1 or 1:2 neutral adducts between **1** and I_2 molecules would provide useful information for the bonding ability of the sulfur atoms. The reaction of **1** with increasing amounts of molecular iodine was carried out in MeCN and in the less polar solvent CH_2Cl_2. In both cases, the formation of red oils, which failed to crystallise on long standing, was observed. The FT-Raman spectra recorded in the ν(I–I) region at **1**/I_2 molar ratios of 1:1 and 1:2 showed an intense peak at 113 cm^{-1} in MeCN and at 110 cm^{-1} in CH_2Cl_2 solution, which are indicative of the formation/presence of the I_3^- species. A further addition of I_2, according to Raman peaks at 113, 146 and 169 cm^{-1} (MeCN) and 113, 146 and 169 cm^{-1} (CH_2Cl_2), led to the formation of complex mixtures.[8]

The reaction of **1** with an equimolar amount of mercury(II) perchlorate or lead(II) nitrate, carried out in MeCN at room temperature, quickly led to the decolouration of the solution with the formation of a mixture of white and brown sticky powders. Conversely, in the reaction with palladium(II) chloride the colour change was not observed, and complex **1** was recovered unreacted when the solution was slowly concentrated in air. Interestingly, when the above reactions were carried out in the presence of aqueous NaOH to obtain a **1**/M/NaOH [M = Hg^{II}, Pb^{II} and Pd^{II} ions] reaction molar ratio of 1:1:2, sticky oils including a thin blue powder were observed in all cases. The addition of aqueous NaOH to a solution of complex **1** (**1**/NaOH, 1:2) in CH_3CN readily afforded a deep-blue solution along with a very thin brown powder.[9] From the concentration of the solution a blue powder was obtained, and subsequent crystallisation from CH_3CN/hexane yielded well-shaped blue crystals with elemental analyses corresponding to the formulation $[Co\{L_{(OS)}\}_2]$ (**2**).

Solid complexes **1** and **2** and their MeCN solutions are easily recognisable because of their green and blue colour, respectively. Visible absorption spectra of these complexes in the range 500–800 nm are reported in Figure 3; in both compounds, the molar intensities of the d–d electronic transition bands [compound **1**: UV/Vis (CH_3CN): λ_{max} (ε, $dm^3\,mol^{-1}\,cm^{-1}$) = 661 (172), 696 (346), 734 (432) nm; com-

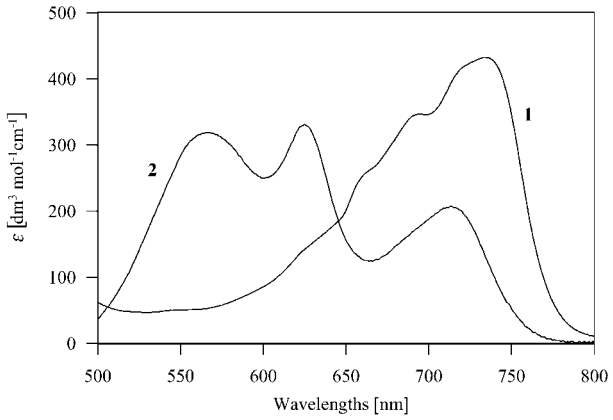

Figure 3. Visible absorption spectra in MeCN of complexes **1** [λ_{max} = 734, 696, 661 (sh) nm] and **2** (λ_{max} = 715, 625, 566 nm).

pound **2**: UV/Vis (CH_3CN): λ_{max} (ε, $dm^3 mol^{-1} cm^{-1}$) 566 (319), 625 (331), 715 (205) nm] are consistent with Co^{II} bound in a tetrahedral or distorted tetrahedral coordination geometry.[10] The absorption spectra in the visible region, taken after the addition of increasing amounts of aqueous NaOH to a solution of **1** in MeCN are reported in Figure 4; from the analysis of the bands at 734 and 566 nm, related to complexes **1** and **2**, respectively, it results that only a partial conversion of **1** into **2** occurs because of the observed concomitant formation of a thin brown powder.[9] The inset to Figure 4 gives evidence of this fact and shows that a near sixfold excess of NaOH over the amount of **1** is necessary to obtain a 55% yield of **2**.

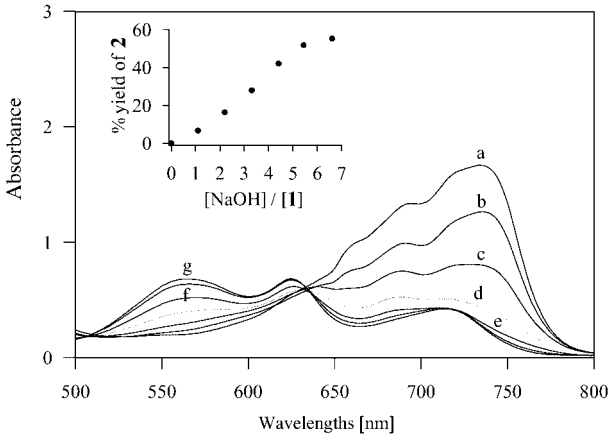

Figure 4. Base-induced conversion of complex **1** into **2**, as monitored by Visible absorption spectroscopy. (a) [Co{$HL_{(OS)}$}$_2I_2$] (**1**), 3.85×10^{-3} M in MeCN, 21 °C; and after the addition of NaOH (1.0 M in water) to realise a NaOH/[**1**] molar ratio of (b) 1.1; (c) 2.2; (d) 3.3; (e) 4.4; (f) 5.5 and (g) 6.6. Inset: percent yield of complex **2**, which results from analysis of the bands at 566 and 734 nm, plotted vs. [NaOH]/[**1**] molar ratios.

The molecular structure of **2** (Figure 5 and Table 1) features a Co^{II} ion in a tetrahedral coordination geometry linked through oxygen and sulfur atoms to two bidentate anionic ligands [$N(OPPh_2)(SPPh_2)$]$^-$. As a result, the metal ion is surrounded by a spirobicyclic {$NP_2(S)O$}Co{$O(S)P_2N$} system, with endocyclic S···O bites of 3.439(4)/3.553(5) Å (see Table 1). The tetrahedral CoO_2S_2 core is slightly distorted and shows X–Co–Y (X, Y = S, O) angles in the range 105.86(17)–115.03(14)°, Co–O/Co–S average distances of 1.980(6)/2.331(3) Å (Table 1) and a Co(1)–S(1)–O(1)/Co(1)–S(2)–O(2) dihedral angle of 86.28(10)°. The Co–X (X = S, O) bond lengths are very close to those reported for various monomeric Co^{II} complexes with tetra- or octahedral coordination geometry,[11] such as [Co{$N(SPPh_2)_2$}$_2$][4b] [av. Co–S 2.335(2) Å], [$Co(OAc)_2$(etu)$_2$],[12a] [Co–S 2.328(3) Å, av. Co–O 1.957(7) Å; etu = ethylenthiourea] and [$Co(acac)_2(py)_2$][12b] [Co–O 2.034(3) Å; acac = acethylacetonate]. As similarly observed in complexes [Mn{$N(OPPh_2)(SPPh_2)$}$_2$][13a] and [Ni{$N(OPR_2)(SPPh_2)$}$_2$] (R = Ph, Me),[13b] no static disorder effects[13c] in the metal-bonded donor-atom sites are present. Close inspection of the structure shows that the two chemically equivalent, nonplanar $CoO(S)P_2N$ rings exhibit different geometries. The Co(1)–S(2)–P(3)–N(2)–P(4)–O(2) ring in fact, is arranged in a pseudochair conformation with P(4) and S(2) in the apices and dihedral angles between the nearly planar Co(1)–P(3)–N(2)–O(2) array [max. dev. from mean plane ±0.040(2) Å] and Co(1)–S(2)–P(3) and O(2)–P(4)–N(2) planes of 42.08(9) and 13.0(3)°, respectively. Co(1)–S(1)–P(1)–N(1)–P(2)–O(1) indeed shows a highly distorted pseudoboat geometry where S(1) and P(2) act as "bow" and "stern" in comparison to the slightly twisted Co(1)–P(1)–N(1)–P(2) plane [max. dev. ±0.119(2) Å], with P(1)–S(1)–Co(1)–N(1)–P(1)–Co(1)–O(1) and N(1)–P(2)–O(1)–N(1)–P(1)–Co(1)–O(1) dihedral angles of 30.92(15) and 17.7(4)°, respectively. As already observed in the related complex [Co{$N(SPPh_2)$}$_2$], some degree of π-electron delocalisation is present on the $CoO(S)P_2N$ rings, as shown by the P–X (X = S, O) average bond lengths, which increase with respect to [$HN(OPPh_2)(SPPh_2)$][14] by 0.071 Å (P–O) and 0.083 Å (P–S), whereas the average N–P distances decrease by 0.104 Å.

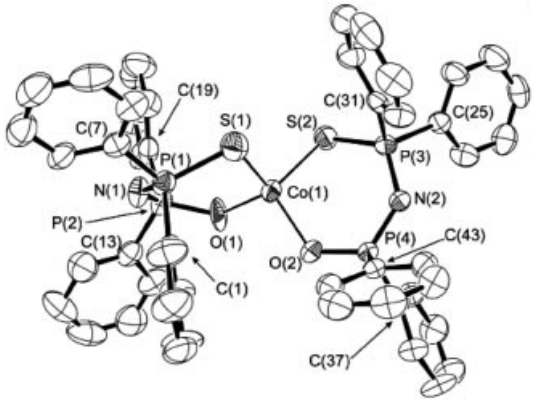

Figure 5. ORTEP drawing and atom-labelling scheme for [Co^{II}{$N(OPPh_2)(SPPh_2)$-*O*,*S*}$_2$] (**2**). Thermal ellipsoids are drawn at 50% probability.

Reactivity of Complex 2

In previous papers it was demonstrated that in complexes of the formula M{$L_{(SS)}$}$_2$ (M = Pd, Cu)[4c,5] it was possible to protonate the metal-bound ligands to form the corresponding cationic complexes in which the S,S′ chelation of the ligands was preserved. As a result of the different set of donor atoms in complex **2**, the protonation of the metal-bound ligands may induce different coordination modes at the metal centre: complexes with CoO_2X_2 or CoS_2X_2 cores and with X being a cobalt-coordinating anion. The formation of the cationic complex [Co{$HL_{(OS)}$}$_2$]$^{2+}$ in which the CoO_2S_2 core is preserved cannot be excluded either. In this study the reactivity of **2** was only tested towards HI to verify the feasibility of this synthetic procedure and the nature of the formed complex. The reaction of **2** in MeCN with increasing amounts of hydroiodic acid (55 wt.-% in water) to reach a **2**/HI molar ratio of 1:4 results in the complete disappearance of the visible band at 566 nm, which is characteristic of complex **2**, and the formation of the pattern of

bands related to the formation of complex **1**. The diagram reporting the conversion of **2** into complex **1** vs. the molar ratios of HI/**2** shows that such a conversion is almost stoichiometric (ca. 92%) when starting with a HI/**2** molar ratio of 2 (Figure 6).

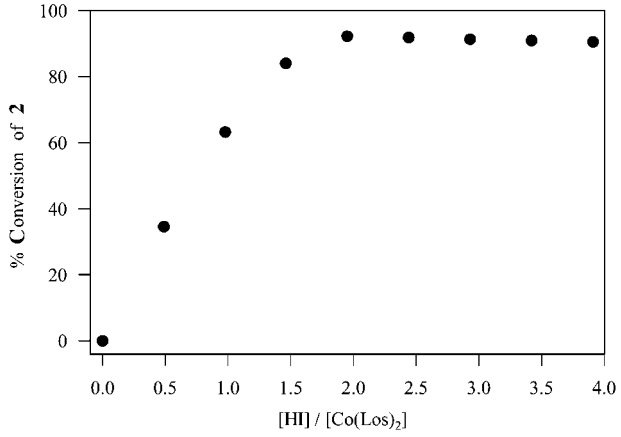

Figure 6. Percent conversion of compound **2** into **1** vs. [HI]/[**2**] molar ratios, which results from analysis of the bands at 566 and 734 nm. $[Co\{L_{(OS)}\}_2]$ (**2**), 7.25×10^{-4} M in MeCN, HI (55% in water), 21 °C. HI/[**2**] molar ratios: 0.00, 0.48, 0.97, 1.46, 1.95, 2.44, 2.93, 3.42, 3.91.

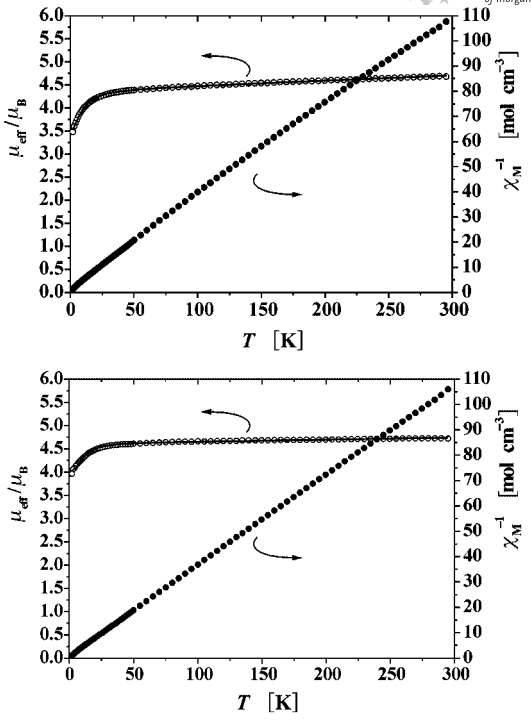

Figure 7. Plots of μ_{eff} (○) and χ_M^{-1}(●) vs. temperature for **1** (top) and **2** (bottom) at 5000 G; the solid lines represent the fitted calculated curve (see text).

Magnetic Studies and Theoretical Calculations

Electronic structures of the new complexes were probed by SQUID measurements and DFT calculations. Magnetic susceptibility measurements were carried out for both complexes at two different magnetic fields in a temperature range from 2.0 to 295 K. No significant field dependence was observed for either of the complexes. The temperature dependence of χ_M^{-1} and the effective magnetic moment μ_{eff} are shown in Figure 7. The value of μ_{eff} is around 4.70 or 4.75 μ_B for **1** or **2**, respectively, at room temperature, which is in the range expected for high-spin (S = 3/2) Co^{II} ions that reside in a tetrahedral environment.[15] The value of μ_{eff} remains almost constant over a large temperature range but drops to around 3.5 μ_B at very low temperatures. This may be attributed to zero-field splitting (ZFS) of the $^4A_2$ ground state, which can be quite large for tetrahedral Co^{II} (although smaller than for five- or six-coordinate Co^{II} ions).[15–18] Magnetic parameters were determined by using a fitting procedure to the spin Hamiltonian for axial ZFS and Zeeman interaction as shown in Equation (2).[19]

$$H = D[S_z^2 - 1/3\,S(S+1)] + g\mu_B \vec{S}\cdot\vec{B} \quad (2)$$

Temperature-independent paramagnetism (*TIP*) was included according to $\chi_{calcd.} = \chi + TIP$. For both complexes slightly better agreement with experimental data was obtained when intermolecular interactions were considered in a mean field approach by using a Weiss temperature Θ.[20,21] Best simulation parameters are g = 2.25, $|D|$ = 12.0 cm^{-1}, $TIP = 1310 \times 10^{-6}$ $cm^3 mol^{-1}$ and Θ = 0.11 K for **1** and g = 2.37, $|D|$ = 11.9 cm^{-1}, $TIP = 541 \times 10^{-6}$ $cm^3 mol^{-1}$ and Θ = 0.66 K for **2**. The $|D|$ parameters for **1** and **2** are almost identical and lie in the upper range of typical values for many tetrahedral Co^{II} compounds (7–12 cm^{-1}).[15,17] ZFS values around –9.5 cm^{-1} were recently found for two other compounds with a tetrahedral $[CoI_2O_2]$ core, whereas larger values D = –12.4 cm^{-1} and D = –16.7 cm^{-1} were reported for $[CoCl_2(PPh_3)_2]$ and $[CoBr_2(PPh_3)_2]$, respectively.[21] The Weiss temperature Θ relates to intermolecular interactions zJ of 0.03 cm^{-1} for **1** and 0.18 cm^{-1} for **2**, where J is the interaction parameter between two nearest neighbour magnetic centres and z is the number of nearest neighbours.[22] Intermolecular interactions are apparently very weak if not negligible for both complexes, and they appear to be even smaller for **1** than for **2**. This confirms that no significant coupling occurs through the H-bonding linkages that constitutes the 1D polymeric array in **1**.

DFT calculations (see Experimental Section) were performed on the anionic model ligands $[N(OPH_2)(SPH_2)]^-$, $L'_{(OS)}$, and $[N(SPH_2)_2]^-$, $L'_{(SS)}$, and on the corresponding neutral Co^{II} complexes $[Co\{N(OPH_2)(SPH_2)\text{-}O,S\}_2]$ (**3**) and $[Co\{N(SPH_2)_2\text{-}S,S'\}_2]$ (**4**). The geometry optimisation of these complexes in their quartet electron configuration with the use of the UB3LYP hybrid functional yields bond lengths and angles very close to the structural ones (Tables S1 and S2, Supporting Information). As regards $L'_{(SS)}$, the optimised bond lengths and angles are reproduced well relative to those previously reported with

Gaussian 94 at the same level of theory.[4b] In Figure 8, the HOMO and LUMO computed for $L'_{(OS)}$ and $L'_{(SS)}$ are depicted. In both compounds, the HOMO is mainly built of the in-plane p atomic orbitals of the sulfur donor atoms, which are negatively charged; the calculated Mulliken charge for $L'_{(OS)}$ are Q_S = –0.582 e, Q_O = –0.578 e and for $L'_{(SS)}$ the calculated charge Q_S = –0.561 e. It is noteworthy that the calculated Q_S charges show similar values, which suggests a similar bonding ability for the P–S groups in the related anionic ligands; the acidity constant values determined experimentally for the $HL_{(OS)}$ and $HL_{(SS)}$ ligands (pK_a = 5.42 and 5.61, respectively) further support this view. The Mulliken charge calculated on the metal centre at the fully relaxed geometry (Figure 9) shows a marked difference in the $Co^{II}O_2S_2$ and $Co^{II}S_4$ cores (Q_{Co} = 0.436 and 0.023 e in **3** and **4**, respectively), which might be the basis for the different reactivities of the two complexes. This is reflected in a different charge distribution on the S–P–N–P–O and S–P–N–P–S elements that constitute the backbones of complexes **3** and **4**, which show markedly different values, mostly related to the P=O and P=S groups.

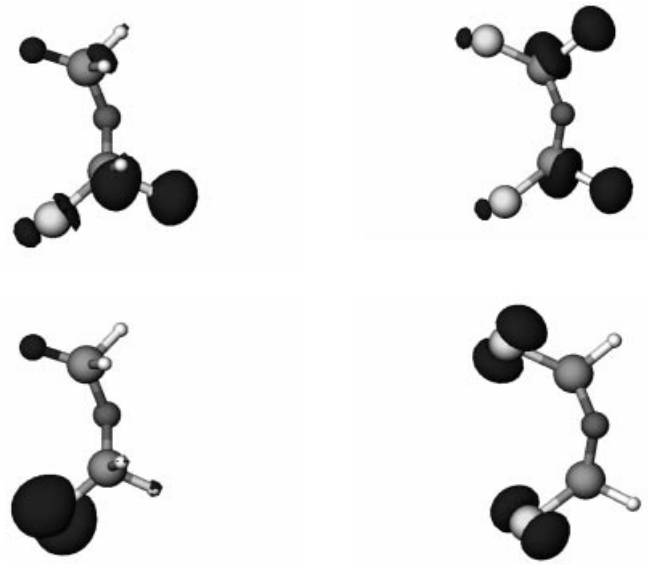

Figure 8. HOMO (bottom row) and LUMO (top row) drawings in $L'_{(OS)}$ (left) and $L'_{(SS)}$ (right). Optimised selected bond lengths and angles: $L'_{(OS)}$: P–S 1.984, P–O 1.504, N–P(O) 1.621, N–P(S) 1.619 Å; P–N–P 128.14°;·$L'_{(SS)}$: P–S 1.980, P–N 1.623 Å; P–N–P 128.20°.

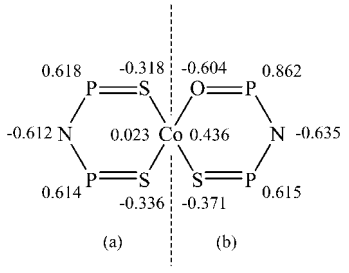

Figure 9. Mulliken charge distribution (e) in model complexes **4** (a) and **3** (b). Hydrogen atoms are omitted for clarity.

Conclusions

The Co^{II} complex $[Co\{[HN(OPPh_2)(SPPh_2)\text{-}O]_2\}I_2]$ (**1**) was synthesised in a single step from the oxidation of cobalt powder by the adduct $HL_{(OS)}{\cdot}I_2$ in Et_2O prepared in situ. The X-ray crystal structure of this complex shows a Co^{II} ion in a tetrahedral coordination environment with the ligands in a neutral form, which has not been previously observed, and the metal ion is bound through the oxygen atoms and two iodide ions, which completes the CoI_2O_2 core. This mode of ligation leaves the $–PPh_2(S)$ groups in a dangling position, which we were unsuccessful in involving in further coordination activity towards "soft" centres. The treatment of **1**, dissolved in MeCN, with NaOH caused the deprotonation of the imido group in the ligands and the formation of $[Co\{[N(OPPh_2)(SPPh_2)\text{-}O,S]_2\}]$ (**2**), in which the Co^{II} ion is found to occupy a tetrahedral coordination environment with a CoO_2S_2 core. The magnetic behaviour of **1** and **2** is consistent with tetrahedral high-spin (S = 3/2) Co^{II} possessing a $^4A_2$ ground state with appreciable ZFS ($|D| \approx 12\ cm^{-1}$). When complex **2** is treated with hydroiodic acid, complex **1** is almost quantitatively reobtained. Comparison of the Mulliken charges at the Co^{II} centres in the CoO_2S_2 and CoS_4 cores reveals that the metal in the latter core is markedly less electropositive (0.437 and 0.023 e, respectively) than the former, which instills different intrinsic reactivity towards nucleophilic agents.

Experimental Section

Materials and instrumentation: Reagents were used as purchased from Aldrich. Diethyl ether was distilled from $LiAlH_4$ shortly before use. IR spectra were measured as KBr (4000–400 cm^{-1}) pellets with a Bruker Equinox 55 FTIR spectrometer. FT-Raman spectra were recorded with a Bruker FRS 100/S Fourier transform Raman spectrometer operating with a diode-pumped Nd:YAG exciting laser emitting at 1064 nm. ^{31}P NMR spectra were recorded with a Varian Unity 300 MHz spectrometer. The pK_a values of the $HL_{(OS)}$ and $HL_{(SS)}$ ligands were determined by NMR spectroscopic measurements according to the guidelines reported in the IUPAC Technical Report.[23] The ^{31}P NMR spectra of 19 different solutions in MeCN/H_2O, 4:1 (5.12×10^{-3} M) and 0.1 M $[(Bu)_4N(NO_3)]$, as supporting electrolyte, at (25.0 ± 0.2) °C were recorded in the pH range 2.5–12.0. The pH values were adjusted by the addition of HCl or NaOH (0.1 or 0.5 M). Peak positions are reported relative to H_3PO_4 (85%) at δ = 0.00 ppm used as external reference in a sealed coaxial tube. pH values were measured with a glass electrode. The experimental data were fitted by a sigmoidal equation with the SigmaPlot software (see Supporting Information, section S3). Visible absorption spectra were measured with a Nicolet Evolution 300 spectrophotometer. Susceptibility measurements were carried out with a Quantum-Design MPMS-5S SQUID magnetometer equipped with a 5 T magnet in the range from 295 to 2 K. The powdered samples were contained in a gel bucket and fixed in a nonmagnetic sample holder. Each raw data file for the measured magnetic moment was corrected for the diamagnetic contribution of the sample holder and the gel bucket. Experimental data were corrected for the underlying diamagnetism by using tabulated Pascal constants (incremental method). Simulations of the experimental magnetic data were performed with full-matrix diagonalisation of zero-field splitting

and Zeeman interaction according to the appropriate Hamiltonian (see text) and including temperature-independent paramagnetism (*TIP*).[24] The ligand $HN(OPPh_2)(SPPh_2)$, $HL_{(OS)}$, was prepared according to ref.[25] Quantum chemical calculations were carried out at the density functional theory (DFT) level by using the NWChem. 4.7 program[26,27] and ECCE 3.2.5.[28] DFT calculations were attempted on $[Co\{[HN(OPh_2)(SPh_2)\text{-}O]_2\}I_2]$, $[Co\{[HN(SPh_2)(OPh_2)\text{-}S]_2\}I_2]$, $[Co\{N(OPh_2)(SPh_2)\text{-}O,S\}_2]$ (**3**) and $[Co\{N(SPh_2)_2\text{-}S,S'\}_2]$ (**4**) by adopting different functionals and basis sets. Unfortunately, notwithstanding the numerous attempts and different types of SCF convergence methods, a combination of functional and basis set capable to allow SCF convergence for all compounds was not found. We report here the results obtained for **3** and **4** by using Schafer, Horn and Ahlrichs all-electron double-ζ basis sets with polarisation function[29] for the ligand atoms, the LanL2DZ basis set along with effective core potentials[30] for Co,[31] with the three-parameter[32] hybrid B3LYP functional (based on the gradient corrected Becke exchange functional[33] along with the Lee, Yang and Parr correlation functional[34]). All calculations were performed on a Pentium 4 workstation running on a Linux Mandriva One 2006 operating system.

$[Co\{HN(OPPh_2)(SPPh_2)\text{-}O\}_2I_2]$ (1). A mixture of $HL_{(OS)}$ (0.100 g, 0.230 mmol) and I_2 (0.058 g, 0.230 mmol) in diethyl ether (200 mL) was stirred at 25 °C under an atmosphere of N_2 until the reagents were completely dissolved. Cobalt metal powder (< 2 μ; 0.014 g, 0.237 mmol) was added while stirring. This was continued at room temperature for ca. 4 d. The resulting emerald green solid was collected by suction filtration, washed with a mixture of CH_2Cl_2/*n*-hexane (1:5) and dried in vacuo. Yield: 0.074 g (26.4%). M.p. > 250 °C. IR (KBr): $\tilde{\nu}$ = 2632 (w), 1436 (vs), 1328 (m), 1312 (s), 1172 (s), 1151 (s), 1129 (s), 1099 (s), 1026 (w), 998 (w), 998 (s), 944 (s), 789 (s), 747 (s), 728 (s), 688 (s), 646 (s), 614 (w), 569 (m), 523 (m), 487 (m) cm^{-1}. UV/Vis (CH_3CN): λ_{max} (ε, $dm^3\,mol^{-1}\,cm^{-1}$) = 661 (172), 696 (346), 734 (432) nm. $C_{48}H_{42}CoI_2N_2O_2P_4S_2$ (1179.57): calcd. C 48.87, H 3.59, N 2.37, S 5.44; found C 49.1, H 3.7, N 2.4, S 5.2.

$[Co\{N(OPPh_2)(SPPh_2)\text{-}O,S\}_2]$ (2). To a stirred solution of compound **1** (0,100 g, 0.084 mmol) dissolved in CH_3CN (25 mL) was slowly added NaOH (1 M, 180 μL, 0.180 mmol). The deep-blue solution was concentrated to separate well-shaped blue crystals that were washed with CH_2Cl_2/*n*-hexane (1:5) and dried in vacuo. Yield: 0.064 g (83%). M.p. 176 °C. IR (KBr): $\tilde{\nu}$ = 3054 (w), 1636 (m), 1482 (w), 1436 (s), 1236 (vs), 1233 (vs), 1178 (s), 1121 (s), 1045 (vs), 1025 (s), 998 (m), 799 (w), 745 (s), 725 (vs), 692 (vs), 618 (w), 575 (vs), 548 (vs), 419 (s), 506 (s) cm^{-1}. UV/Vis (CH_3CN): λ_{max} (ε, $dm^3\,mol^{-1}\,cm^{-1}$) = 566 (319), 625 (331), 715 (205) nm. $C_{48}H_{40}CoN_2O_2P_4S_2$ (923.75): calcd. C 62.41, H 4.36, N 3.03, S 6.94; found C 63.0, H 4.4, N 3.0, S 7.1.

X-ray Crystallography: Intensities were corrected for Lorentz-polarisation effects and absorption effects by employing multiscan SADABS for compound **1**,[35] and ψ-scan[36a] for compound **2**. Both structures were solved by direct methods (SIR-97)[36b] and refined on F_o^2 with the SHELXL-97[36c] program (WINGX suite[36d]). All non-hydrogen atoms were refined with anisotropic displacement parameters. All H atoms, seen on the ΔF maps, were introduced in the structure model. For compound **1** they were allowed to ride on the corresponding C atoms, whereas for compound **2** they were refined with isotropic displacement parameters. Alternative element type assignments to the donor atoms of the chelating ligands were carefully tested, but led to unphysical variation of displacement parameters across the ligand and discarded. The maximum and minimum residual electron density on the final ΔF map are 1.344 and –1.050 e $Å^{-3}$, respectively for compound **1** and 0.527 and –0.447 e $Å^{-3}$ for compound **2**.

CCDC-641240 and -641241 contain the supplementary crystallographic data for this paper. These data can be obtained free of charge from The Cambridge Crystallographic Data Centre via www.ccdc.cam.ac.uk/data_request/cif.

Crystal data for 1: $C_{48}H_{42}CoI_2N_2O_2P_4S_2$, M = 1179.57, orthorhombic, a = 21.892(2) Å, b = 18.590(2) Å, c = 24.046(2) Å, U = 9786.1(16) $Å^3$, T = 294(2) K, space group *P*bca (no. 61), Z = 8, μ = (Mo-K_α) 1.868 mm^{-1}. 85740 reflections (9660 unique) were collected at room temperature in the range $3.22 \le 2\theta \le 52.20°$ by employing a 0.10 × 0.10 × 0.05 mm crystal mounted on a Siemens SMART CCD diffractometer. 5768 reflections (R_{int} = 0.0807), final R_1 [wR_2] values of 0.0506 [0.1306] on $I > 2\sigma(I)$ [all data], with GoF = 0.954 for 550 parameters.

Crystal data for 2: $C_{48}H_{40}CoN_2O_2P_4S_2$, M = 923.75, monoclinic, a = 12.511(2) Å, b = 18.272(5) Å, c = 19.599(3) Å, β = 100.495(10)°, U = 4405.3(16) $Å^3$, T = 298(2) K, space group $P2_1/c$ (no. 14), Z = 4, μ = (Mo-K_α) 0.671 mm^{-1}. 7551 reflections (6064 unique) were collected at room temperature in the range $4.22 \le 2\theta \le 46.00°$ by employing a 0.26 × 0.22 × 0.08 mm crystal mounted on a P4RA Siemens automatic diffractometer. 7548 reflections (R_{int} = 0.0563), final R_1 [wR_2] values of 0.0606 [0.1471] on $I > 2\sigma(I)$ [all data], with GoF = 1.020 for 692 parameters and 4 restraints.

Supporting Information (see footnote on the first page of this article): Optimised geometries of complexes **3** and **4** in Cartesian orthogonal coordinate format, as derived from DFT calculations, and pK_a determination of $HN(OPPh_2)(SPPh_2)$ and $HN(SPPh_2)(SPPh_2)$.

Acknowledgments

Thanks are expressed to Prof. Antonio C. Fabretti (Dipartimento di Chimica, Università di Modena) for helpful discussions and to the "Centro Interdipartimentale Grandi Strumenti (C.I.G.S.)" of the University of Reggio Emilia for providing P4-RA Siemens X-ray equipment. Financial support from the National University Research Council (CNCSIS, Romania; Research project No. A-1456/2007) is greatly appreciated.

[1] a) F. Bigoli, P. Deplano, M. L. Mercuri, M. A. Pellinghelli, G. Pintus, A. Serpe, E. F. Trogu, *Chem. Commun.* **1998**, 2351–2352; b) F. Bigoli, M. C. Cabras, P. Deplano, M. L. Mercuri, L. Marchiò, A. Serpe, E. F. Trogu, *Eur. J. Inorg. Chem.* **2004**, *5*, 960–963; c) G. L. Abbati, M. C. Aragoni, M. Arca, F. A. Devillanova, C. Fabretti, A. Garau, F. Isaia, V. Lippolis, G. Verani, *Dalton Trans.* **2003**, 1515–1519; d) M. C. Aragoni, M. Arca, M. B. Carrea, F. Demartin, F. A. Devillanova, A. Garau, F. Isaia, V. Lippolis, G. Verani, *Eur. J. Inorg. Chem.* **2004**, 4660–4668; e) M. C. Aragoni, M. Arca, M. B. Carrea, F. Demartin, F. A. Devillanova, A. Garau, F. Isaia, V. Lippolis, M. Marcelli, C. Silvestru, G. Verani, *Eur. J. Inorg. Chem.* **2005**, 589–596.

[2] a) M. C. Aragoni, M. Arca, F. A. Devillanova, A. Garau, F. Isaia, V. Lippolis, G. Verani, *Coord. Chem. Rev.* **1999**, *184*, 271–290; b) M. C. Aragoni, M. Arca, F. Demartin, F. A. Devillanova, A. Garau, F. Isaia, V. Lippolis, G. Verani, *Trends in Inorg. Chem.* **1999**, *6*, 1–18.

[3] V. Lippolis, F. Isaia, *Handbook of Chalcogen Chemistry* (Ed.: F. A. Devillanova), RSC, Cambridge, UK, **2007**, ch. 8.2, pp. 477–496.

[4] a) M. Arca, F. A. Devillanova, A. Garau, F. Isaia, V. Lippolis, G. Verani, G. L. Abbati, A. Cornia, *Z. Anorg. Allg. Chem.* **1999**, *625*, 517–520; b) M. C. Aragoni, M. Arca, A. Garau, F. Isaia, V. Lippolis, G. Abbati, C. Fabretti, *Z. Anorg. Allg. Chem.*

2000, *626*, 1454–1459; c) G. L. Abbati, M. C. Aragoni, M. Arca, C. Fabretti, F. A. Devillanova, A. Garau, F. Isaia, V. Lippolis, G. Verani, *J. Chem. Soc. Dalton Trans.* **2001**, 1105–1110.
[5] M. C. Aragoni, M. Arca, M. B. Carrea, F. Demartin, F. A. Devillanova, A. Garau, M. B. Hursthouse, F. Isaia, V. Lippolis, G. Verani, *Eur. J. Inorg. Chem.* **2006**, *1*, 200–206.
[6] I. Haiduc, *Comprehensive Co-ordination Chemistry II: From Biology to Nanotechnology* (Ed.: A. B. P. Lever), Elsevier, Amsterdam **2003**, vol. 1, pp. 323–347.
[7] a) P. T. Ndifon, C. A. McAuliffe, A. G. Mackie, R. G. Pritchard, *Inorg. Chim. Acta* **1998**, *282*, 25–29; b) S. K. Bauer, C. J. Wilis, N. C. Payne, *Acta Crystallogr., Sect. C: Cryst. Struct. Commun.* **1995**, *51*, 586–588; c) S. A. Cotton, V. Franckevicius, J. Fawcett, *Transition Met. Chem.* **2002**, *27*, 38–41.
[8] A. J. Blake, F. A. Devillanova, R. O. Gould, W.-S. Lee, V. Lippolis, S. Parsons, C. Radek, M. Schroder, *Chem. Soc. Rev.* **1998**, *27*, 195–216.
[9] This solid was insoluble in most common organic solvents and in water. Elemental analyses: C 9.4, H 2.1.
[10] F. A. Cotton, D. M. L. Goodgame, M. Goodgame, *J. Am. Chem. Soc.* **1961**, *83*, 4690–4699.
[11] a) L. M. Gilby, B. Piggott, *Polyhedron* **1999**, *18*, 1077–1082; b) C. Silvestru, R. Rosler, J. E. Drake, J. Yang, G. Espinosa-Perez, I. Haiduc, *J. Chem. Soc. Dalton Trans.* **1998**, 73–78; c) C. Silvestru, R. Rosler, I. Haiduc, R. Cea-Olivares, G. Espinosa-Perez, *Inorg. Chem.* **1995**, *34*, 3352–3354.
[12] a) E. M. Holt, S. L. Holt, K. J. Watson, *J. Am. Chem. Soc.* **1970**, *92*, 2721–2724; b) R. C. Elder, *Inorg. Chem.* **1968**, *7*, 1117–1123.
[13] a) I. Szekely, C. Silvestru, J. E. Drake, G. Balasz, S. I. Farcas, I. Haiduc, *Inorg. Chim. Acta* **2000**, *299*, 247–252; b) A. Silvestru, D. Bîlc, R. Rösler, J. E. Drake, I. Haiduc, *Inorg. Chim. Acta* **2000**, *305*, 106–110; c) M. B. Robin, P. Day, *Adv. Inorg. Chem. Radiochem.* **1967**, *10*, 247–422.
[14] J. Yang, J. E. Drake, S. Hernandez-Ortega, R. Rösler, C. Silvestru, *Polyhedron* **1997**, *16*, 4061–4071.
[15] R. L. Carlin, *Magnetochemistry*, Springer, Berlin, Heidelberg, **1986**.
[16] R. L. Carlin, *Science* **1985**, *227*, 1291–1295.
[17] M. W. Makkinen, M. B. Yim, *Proc. Natl. Acad. Sci. USA* **1981**, *78*, 6221–6225.
[18] Because of strong paramagnetic anisotropy, orientation effects were observed when higher external magnetic fields were applied or when a nonpowdered crystalline material was used (partial alignment of the crystals with the applied field because of a dominance of the parallel susceptibility over the perpendicular component).
[19] D is the axial ZFS parameter, μ_B is the Bohr magneton and g is the Landé factor. Inclusion of a rhombic E term in the ZFS leads to very low values for the rhombic distortion ($E/D < 0.01$).
[20] O. Kahn, *Molecular Magnetism*, VCH, Weinheim, **1993**.
[21] T. Avilés, A. Dinis, J. O. Gonçalves, V. Félix, M. J. Calhorda, A. Prazeres, M. G. B. Drew, H. Alves, R. T. Henriques, V. Da Gama, P. Zanello, M. Fontani, *J. Chem. Soc. Dalton Trans.* **2002**, 4595–4602.
[22] Weiss temperature defined as $\Theta = zJS(S + 1)/3k$.
[23] K. Popov, H. Rönkkömäki, L. H. J. Lajunen, *Pure Appl. Chem.* **2006**, *78*, 663–675.
[24] E. Bill, *julX Program*, Max-Planck Institute for Bioinorganic Chemistry, Mülheim, Ruhr, Germany.
[25] A. Schmidpeter, H. Groeger, *Chem. Ber.* **1967**, *100*, 3979–3991.
[26] E. Aprà, T. L. Windus, T. P. Straatsma, E. J. Bylaska, W. de Jong, S. Hirata, M. Valiev, M. Hackler, L. Pollack, K. Kowalski, R. Harrison, M. Dupuis, D. M. A. Smith, J. Nieplocha, V. Tipparaju, M. Krishnan, A. A. Auer, E. Brown, G. Cisneros, G. Fann, H. Fruchtl, J. Garza, K. Hirao, R. Kendall, J. Nichols, K. Tsemekhman, K. Wolinski, J. Anchell, D. Bernholdt, P. Borowski, T. Clark, D. Clerc, H. Dachsel, M. Deegan, K. Dyall, D. Elwood, E. Glendening, M. Gutowski, A. Hess, J. Jaffe, B. Johnson, J. Ju, R. Kobayashi, R. Kutteh, Z. Lin, R. Littlefield, R. X. Long, B. Meng, T. Nakajima, S. Niu, M. Rosing, G. Sandrone, M. Stave, H. Taylor, G. Thomas, J. van Lenthe, A. Wong, Z. Zhang, *NWChem: A Computational Chemistry Package for Parallel Computers (version 4.7)*, Pacific Northwest National Laboratory, Richland, Washington, **2005**.
[27] R. A. Kendall, R. E. Aprà, D. E. Bernholdt, E. J. Bylaska, M. Dupuis, G. I. Fann, R. J. Harrison, J. Ju, J. A. Nichols, J. Nieplocha, T. P. Straatsma, T. L. Windus, A. T. Wong, *Comput. Phys. Commun.* **2000**, *128*, 260–283.
[28] G. Black, B. Didier, T. Elsethagen, D. Feller, D. Gracio, M. Hackler, S. Havre, D. Jones, E. Jurrus, T. Keller, C. Lansing, S. Matsumoto, B. Palmer, M. Peterson, K. Schuchardt, E. Stephan, L. Sun, H. Taylor, G. Thomas, E. Vorpagel, T. Windus, C. Winters, *Ecce: A Problem Solving Environment for Computational Chemistry (version 3.2.5)*, Pacific Northwest National Laboratory, Richland, Washington, **2006**.
[29] A. Schafer, H. Horn, R. Ahlrichs, *J. Chem. Phys.* **1992**, *97*, 2571–2576.
[30] P. J. Hay, W. R. Wadt, *J. Chem. Phys.* **1985**, *82*, 284–298.
[31] Basis sets were obtained from the Extensible Computational Chemistry Environment Basis Set Database (version 02/25/04), as developed and distributed by the Molecular Science Computing Facility, Environmental and Molecular Sciences Laboratory, which is part of the Pacific Northwest Laboratory, P. O. Box 999, Richland, Washington 99352, USA, and funded by the U. S. Department of Energy. The Pacific Northwest Laboratory is a multiprogram laboratory operated by Battelle Memorial Institute for the U. S. Department of Energy under contract DE–AC06–76RLO 1830.
[32] A. D. Becke, *J. Chem. Phys.* **1993**, *98*, 5648–5652.
[33] A. D. Becke, *Phys. Rev. A* **1988**, *38*, 3098–3100.
[34] C. Lee, W. Yang, R. G. Parr, *Phys. Rev. B* **1988**, *37*, 785–789.
[35] *SADABS: Area–Detector Absorption Correction*, Siemens Industrial Automation, Inc., Madison, WI, **1996**.
[36] a) A. C. T. North, D. C. Phillips, F. S. Mathews, *Acta Crystallogr., Sect. A* **1968**, *24*, 351–359; b) A. Altomare, M. C. Burla, M. Camalli, G. L. Cascarano, C. Giacovazzo, A. Guagliardi, A. G. G. Moliterni, G. Polidori, R. Spagna, *J. Appl. Crystallogr.* **1999**, *32*, 115–119; c) G. M. Sheldrick, *SHELX97: Programs for Crystal Structure Analysis (Release 97–2)*, University of Göttingen, Germany, **1998**; d) L. J. Farrugia, *J. Appl. Crystallogr.* **1999**, *32*, 837–838.

Received: April 23, 2007
Published Online: August 20, 2007

